Online Center of Mass and Momentum Estimation for a Humanoid Robot Based on Identification of Inertial Parameters

Kenya Mori[1,2], Ko Ayusawa[1] and Eiichi Yoshida[1,2]

Abstract— **In this paper, we present a real-time method for identification of the inertial parameters of a humanoid robot and an estimation of its center-of-mass (CoM) and linear and angular momentum. CoM and momentum are important for whole-body motion generation of a humanoid robot and can be used as an indicator of motion planning. Because they are affected by modeling errors and inertia changes (e.g., due to object grasping), it is important to estimate them online. The proposed method has the advantage of being based only on the internal sensors. We verified the effectiveness of the proposal method by applying it to a humanoid robot.**

I. INTRODUCTION

Humanoid robots are made to resemble human body dynamics; therefore, they have the advantage of adapting to human infrastructure to work in our society. However, humanoids have a large degree of freedom (DOF) and a complex system, leading to difficulties in generating their motions. Many types of motion generation methods for humanoids have been studied thus far. Some research has focused on whole-body center-of-mass (CoM) [1][2], and others have used not only CoM but also total momentum [3][4][5]. As an example of using the dynamics of momentum for motion generation, Kajita et al. realized kick motion [3]. They set the reference linear momentum (LM) and angular momentum (AM) and commanded a robot to realize those momenta by controlling joint velocities. Dai et al. achieved high-grade exercises, such as an aerial ladder and a salmon ladder, in simulation using CoM acceleration and a rate of change of momentum as indicators in the nonlinear programming [4]. Those motions cannot be performed on real robots unless the modeling error is sufficiently small. Moreover, when the mass property changes during object grasping, the risk of falling down increases. We, therefore, aimed to develop a whole-body CoM and momentum estimation method that is robust against modeling errors and mass property changes upon moving. Our method is based on an online identification technique.

In the robotics field, identification methods of the dynamic parameter using recorded robot motion data have been studied [6][7]. One aim of these studies is the identification of the link mass, the first mass moment (related to the CoM), and the inertia matrix, which are together called inertia parameters. For legged robots, including a humanoid robot, identification using unactuated dynamics of the base link has been proposed [8]. This method uses joint angles, inertial measurement, external forces, and their differentials, which are signals available from sensors embedded in bipedal robots of a standard composition. Although online identification for humanoid robots has not yet been established, some studies have applied this method for human body segment identification and executed it in real-time [9]. Considering the previous work of humans, we propose a method to estimate the whole-body CoM and momentum via sequential inertial parameter identification.

The difference between online identification of a human versus a humanoid can be summarized as follows: (1) The global position and attitude of a robot cannot be directly obtained. (2) Robots can use only internal sensors, which means that they cannot detect pure external forces. (3) Robots have limited computing resources because they must execute not only state estimation but also motion control. Issue (1) can be addressed by expressing the equation of motion with respect to the local coordinate for identification [10]. To deal with the other issues, in this study, we (1) divided all link chains into multiple link segments and (2) made an online identification system that is lightweight and runs at a high speed.

Some investigations have studied CoM estimation for a humanoid robot. Masuya et al. fused CoM-ZMP dynamics and Kinematics information by using Kalman filter for CoM estimation and proved the advantage of their method by comparing several related methods in simulation [11]. Piperakis et at. constructed an estimator of CoM and external forces according to the CoM-ZMP model and evaluated the estimator by using the real robot [12]. Carpentier et al. developed a high-performance CoM observer combining some of the computation CoM by a complementary filter and applied the observer to a human who is walking on a treadmill [13]. Rotella et al. constructed an observer to estimate the CoM, LM, and AM using CoM dynamics, which is robust against modeling error (offset) for intentional attachment [14]. However, it has not been validated on a real robot.

In this paper, we propose a novel framework that provides an estimation of CoM, LM, and AM without the need to construct an individual observer because novel framework is based on the identification of inertial parameters. In addition, the framework can deal with dynamic inertia changes. The contributions of this study compared with previous methods include the following: (1) Separation of link segments whose

*This work was partly supported by JSPS Grant-in-Aid for Scientific Research (A) Number 17H00768, and by JSPS Grant-in-Aid for Scientific Research (B) Number 18H03315.

K. Mori, K. Ayusawa and E. Yoshida are with [1]CNRS-AIST JRL (Joint Robotics Laboratory), UMI3218/RL, Tsukuba, Japan.

K. Mori and E. Yoshida are with [2]University of Tsukuba, Japan. Corresponding author: K. Mori s1720868@s.tsukuba.ac.jp

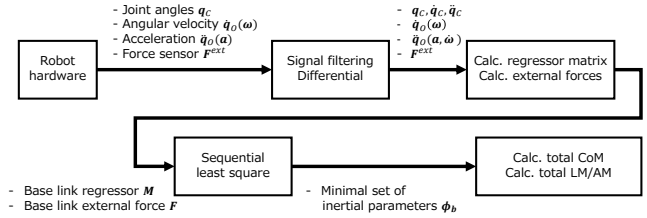

Fig. 1. Flowchart of the proposed method

boundaries are formed by a force sensor. By the separation, the identification system can handle many contact situations. (2) A novel computational framework for inertial parameter identification that uses a sequential least squares method for fast implementation.

This paper is organized as follows. Section II describes the inertial parameter identification method and show solutions for the problem of the online identification for a humanoid. Section III presents the estimation results in the dynamical simulation. Section IV provides the experimental results for validating the proposed method through detection of additional weight of the robot. Finally, conclusions are presented.

II. SEQUENTIAL INERTIAL PARAMETER IDENTIFICATION

Inertial parameters for a multibody system, such as a manipulator, can be estimated using regression analysis because the equation of motion can be written linearly with respect to the inertial parameters. However, the sequential least squares method is often used for the online identification problem. We, therefore, propose a combination of these methods as illustrated in Fig. 1.

A. Equations of motion for humanoid robots

The equations of motion for humanoid robots that have n links, N_J degrees of freedom and N_c contact points is expressed in (1) [15].

$$\begin{bmatrix} \boldsymbol{H}_{O1}\boldsymbol{H}_{O2} \\ \boldsymbol{H}_{C1}\boldsymbol{H}_{C2} \end{bmatrix} \begin{bmatrix} \ddot{\boldsymbol{q}}_O \\ \ddot{\boldsymbol{q}}_C \end{bmatrix} + \begin{bmatrix} \boldsymbol{b}_O \\ \boldsymbol{b}_C \end{bmatrix} = \begin{bmatrix} \boldsymbol{0} \\ \boldsymbol{\tau} \end{bmatrix} + \sum_{i=1}^{N_c} \begin{bmatrix} \boldsymbol{J}_{Oi}^T \\ \boldsymbol{J}_{Ci}^T \end{bmatrix} \boldsymbol{F}_i^{ext} \tag{1}$$

where

- $\boldsymbol{H}_{jk} (j = O, C, k = 1, 2)$ is the inertia matrix,
- $\boldsymbol{q}_O \in \boldsymbol{R}^6$ is the position and the attitude of the floating base,
- $\boldsymbol{q}_C \in \boldsymbol{R}^{N_J - 6}$ is the column vector of joint angles,
- $\boldsymbol{b}_j \in \boldsymbol{R}^{N_J}$ is the column vector including the Coriolis, the gravity, and the centrifugal force,
- $\boldsymbol{\tau} \in \boldsymbol{R}^{N_J - 6}$ is the column vector of the joint torques,
- $\boldsymbol{J} = \begin{bmatrix} \boldsymbol{J}_{Oi} \\ \boldsymbol{J}_{Ci} \end{bmatrix} \in \boldsymbol{R}^{N_J \times 6}$ represents the Jacobian matrices of the contact position i and the orientation of the contact link i,
- $\boldsymbol{F}_i^{ext} \in \boldsymbol{R}^6$ is the external wrench at contact link i.

(1) can be rewritten linearly with respect to each link mass, the first mass moment and the element of the inertia matrix[6], as

$$\begin{bmatrix} \boldsymbol{Y}_O \\ \boldsymbol{Y}_C \end{bmatrix} \boldsymbol{\phi} = \begin{bmatrix} \boldsymbol{0} \\ \boldsymbol{\tau} \end{bmatrix} + \sum_{i=1}^{N_c} \begin{bmatrix} \boldsymbol{J}_{Oi}^T \\ \boldsymbol{J}_{Ci}^T \end{bmatrix} \boldsymbol{F}_i^{ext} \tag{2}$$

where

- $\boldsymbol{Y_O} \in \boldsymbol{R}^{6 \times 10n}$ is a coefficient matrix called a regressor. It is related to the floating base and computed using the base link velocity (linear and, angler), joint angles, and that differentiation,
- $\boldsymbol{Y_C} \in \boldsymbol{R}^{N_J - 6 \times 10n}$ is a regressor matrix that relates to each joint,
- $\boldsymbol{\phi} = \begin{bmatrix} \boldsymbol{\phi}_1^T, \boldsymbol{\phi}_2^T, \ldots, \boldsymbol{\phi}_j^T, \ldots, \boldsymbol{\phi}_n^T \end{bmatrix}^T \in \boldsymbol{R}^{10n}$ represents the column vector of the inertial parameters. The inertial parameters of link j are defined as follows:

$$\begin{aligned} \boldsymbol{\phi}_j = [&m_j, \ m_j c_{jx}, \ m_j c_{jy}, \ m_j c_{jz}, \\ &I_{jxx}, \ I_{jyy}, \ I_{jzz}, \ I_{jyz}, \ I_{jzx}, \ I_{jxy}]^T \end{aligned} \tag{3}$$

Then, m_j , c_{j*}, and I_{j**} are the link mass, the distance between the joint local coordinates with the CoM and the elements of the inertia matrix, respectively.

Inertial parameters expressed as $\boldsymbol{\phi}$ are redundant when calculating the kinematics or dynamics because they contain parameters not included in the dynamics model. The identifiable parameters are called base parameters or a minimal set of parameters [16][17]. Let $\boldsymbol{\phi}_b$ be the base parameters, and $N_b (< 10n)$ be the number of base parameters. The relation of $\boldsymbol{\phi}$ and $\boldsymbol{\phi}_b$ can be represented by (4).

$$\boldsymbol{\phi}_b = \boldsymbol{Z}\boldsymbol{\phi} \tag{4}$$

where, $\boldsymbol{Z} \in \boldsymbol{R}^{N_b \times 10n}$ is the composition matrix. An analytical method of computing the matrix $\boldsymbol{Z}$ for humanoid robots has been established [8]. By using $\boldsymbol{\phi}_b$, (2) can be rewritten as (5), where $\boldsymbol{Y}_{Ob} \in \boldsymbol{R}^{6 \times N_b}$ is a regressor matrix with respect to $\boldsymbol{\phi}_b$.

$$\begin{bmatrix} \boldsymbol{Y}_{Ob} \\ \boldsymbol{Y}_{Cb} \end{bmatrix} \boldsymbol{\phi}_b = \begin{bmatrix} \boldsymbol{0} \\ \boldsymbol{\tau} \end{bmatrix} + \sum_{i=1}^{N_c} \begin{bmatrix} \boldsymbol{J}_{Oi}^T \\ \boldsymbol{J}_{Ci}^T \end{bmatrix} \boldsymbol{F}_i^{ext} \tag{5}$$

The upper part of (5) does not include the joint torques. Thus, it can be calculated without measuring the torques. In addition, we confirmed that the minimal set of inertial parameters for the whole-body dynamics is exactly equal to the minimal set for the base-link dynamics[8]. Finally, the identification equation can be written with respect to the local base link coordinate. Therefore, it does not depend on the base link position or attitude of the world coordinate and can be calculated using only the robot's proprioceptive sensors (IMU, force sensors, and encoders)[10].

$$\boldsymbol{Y}_{Ob}\boldsymbol{\phi}_b = \sum_{i=1}^{N_c} \boldsymbol{J}_{Oi}^T \boldsymbol{F}_i^{ext} \tag{6}$$

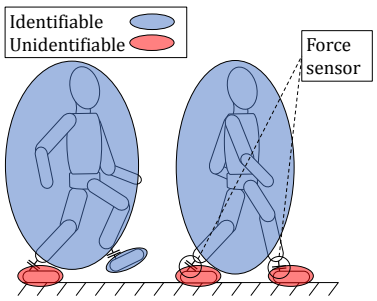

Fig. 2. The contact state causes changes in several identifiable links

B. Division of the dynamic model using force sensor signals

In this section, we describe the division of the dynamic model into multiple segments by considering the state of the force sensor installed in the robot. Legged robots usually contact the environment through force sensors. Because the measurable external force changes due to the sensor arrangement, it is necessary to consider these differences. Figure 2 shows the contact situation when the humanoid robot walks. The entire kinematic chain is divided into three for the two foot force sensors. Blue links do not contact with the environment, whereas the red one contacts directly with the environment. Because red segments cannot detect the external force from the floor, those are unidentifiable. Thus, it is necessary to consider the contact situations and divide the equation of motion. Assuming that the force sensor is mounted on both feet, (6) can be described as follows.

$$\begin{cases} {}^{b}\boldsymbol{Y}_{Ob}{}^{b}\phi_b = {}^{b}\boldsymbol{J}_{rfs}^{T}\boldsymbol{F}_{rfs} + {}^{b}\boldsymbol{J}_{lfs}^{T}\boldsymbol{F}_{lfs} & \text{(7a)} \\ {}^{r}\boldsymbol{Y}_{Ob}{}^{r}\phi_b = {}^{r}\boldsymbol{J}_{O1}^{T}\boldsymbol{F}_{O1}^{ext} + {}^{r}\boldsymbol{J}_{rfs}^{T}\boldsymbol{F}_{rfs} & \text{(7b)} \\ {}^{l}\boldsymbol{Y}_{Ob}{}^{l}\phi_b = {}^{l}\boldsymbol{J}_{O2}^{T}\boldsymbol{F}_{O2}^{ext} + {}^{l}\boldsymbol{J}_{lfs}^{T}\boldsymbol{F}_{lfs} & \text{(7c)} \end{cases}$$

where,

- ${}^{j}\boldsymbol{Y}_{Ob}(j = b, r, l)$ represents the regress matrices for the three kinematic sub-chains equations: the trunk-side link segments, the right foot, and the left foot,
- ${}^{j}\phi_b$ is the minimal set of inertial parameters that correspond to the link segments of each sub-chain,
- ${}^{j}\boldsymbol{J}_{kfs}(k = r, l)$ represents the Jacobian matrices of the position and orientation of force sensor k with respect to the generalized coordinates of sub-chain j,
- ${}^{j}\boldsymbol{J}_{Op}(p = 1, 2)$ represents the Jacobian matrices of the contact points and the orientations with respect to the generalized coordinates of sub-chain j,
- $\boldsymbol{F}_{kfs}$ is the force/moment (or wrench) acting on force sensor k,
- $\boldsymbol{F}_{Op}$ is the set of external forces.

Because $\boldsymbol{F}_{O1}$ and $\boldsymbol{F}_{O2}$ are not detected, (7b) and (7c) can only distinguish the swing phase. In the following discussion, (7a) is expressed as follows.

$$\boldsymbol{M}\phi_b = \boldsymbol{F} \tag{8}$$

C. Online estimation using the weighted least squares method

When each observed signal is represented by a different unit of measure or has a different signal/noise ratio, the weighted least squares method performs better performance than the least squares method. We, therefore, use the weighted least squares method for online identification.The observation error is defined as $\varepsilon \in \boldsymbol{R}^{6\times1}$ at time t, and (8) can be written as follows.

$$\boldsymbol{F}_t = \boldsymbol{M}_t\phi_{\boldsymbol{b}|t} + \varepsilon \tag{9}$$

From all observations until t, the estimation value $\hat{\phi}_{\boldsymbol{b}|t}$ to minimize ε is calculated using the least squares method.

$$\hat{\phi}_{\boldsymbol{b}|t} = \boldsymbol{H}_t{}^{-1}\boldsymbol{B}_t \tag{10}$$

where $\boldsymbol{H}_t$ and $\boldsymbol{B}_t$ are defined below.

$$\boldsymbol{H}_t = \boldsymbol{H}_{t-1} + \boldsymbol{M}_t^{T}\boldsymbol{\Sigma}_t\boldsymbol{M}_t \tag{11}$$

$$\boldsymbol{B}_t = \boldsymbol{B}_{t-1} + \boldsymbol{M}_t^{T}\boldsymbol{\Sigma}_t\boldsymbol{F}_t \tag{12}$$

Weight matrix $\boldsymbol{\Sigma}_t \in \boldsymbol{R}^{6\times6}$ at time t is calculated according to reference to[9].

$$\boldsymbol{\Sigma}_t = \begin{bmatrix} \frac{1}{\sigma_{1|t}} & 0 & 0 & 0 & 0 & 0 \\ 0 & \frac{1}{\sigma_{2|t}} & 0 & 0 & 0 & 0 \\ 0 & 0 & \frac{1}{\sigma_{3|t}} & 0 & 0 & 0 \\ 0 & 0 & 0 & \frac{1}{\sigma_{4|t}} & 0 & 0 \\ 0 & 0 & 0 & 0 & \frac{1}{\sigma_{5|t}} & 0 \\ 0 & 0 & 0 & 0 & 0 & \frac{1}{\sigma_{6|t}} \end{bmatrix} \tag{13}$$

$$\sigma_{i|t} = \hat{\phi}_{\boldsymbol{b}|t-1}^{T}(\boldsymbol{A}_{i|t}\hat{\phi}_{\boldsymbol{b}|t-1} - 2\boldsymbol{B}_{i|t}) + C_{i|t} \tag{14}$$

$$\boldsymbol{A}_{i|t} = \boldsymbol{A}_{i|t-1} + \boldsymbol{m}_{i|t}^{T}\boldsymbol{m}_{i|t} \tag{15}$$

$$\boldsymbol{B}_{i|t} = \boldsymbol{B}_{i|t-1} + \boldsymbol{m}_{i|t}^{T}f_{i|t} \tag{16}$$

$$C_{i|t} = C_{i|t-1} + {f_{i|t}}^{2} \tag{17}$$

where the i-th row element in $\boldsymbol{M}_t$ is expressed by $\boldsymbol{m}_{i|t}$, and the i-th row element in $\boldsymbol{F}_t$ is expressed as $f_{i|t}$; in addition, the initial values of $\boldsymbol{A}_{*|0}$, $\boldsymbol{B}_{*|0}$, and $\boldsymbol{C}_{*|0}$ are set to appropriate a zero matrix.

III. SIMULATIONS

To evaluate the proposed method, the total CoM, LM, and AM were estimated using a dynamic simulation with humanoid robot HRP-4 [18]. The dynamic simulations have been performed by Choreonoid [19] on an Intel(R) Core(TM) i7-6820HQ CPU. HRP-4 had 37 DOF in its joints, and the number of identifiable parameters in it was $N_b = 255$. This is the same number of minimal set of inertial parameters in (7a). As the motion for verification, the robot executed a motion that included a chest segment exciting motion [20] (10 s), a squat motion (20 s), and an arm exciting motion (10 s). The total time, including the interpolation between motions, was approximately 47 s. The simulation was executed by 1000 Hz, and the control rate of the robot was 200 Hz. We

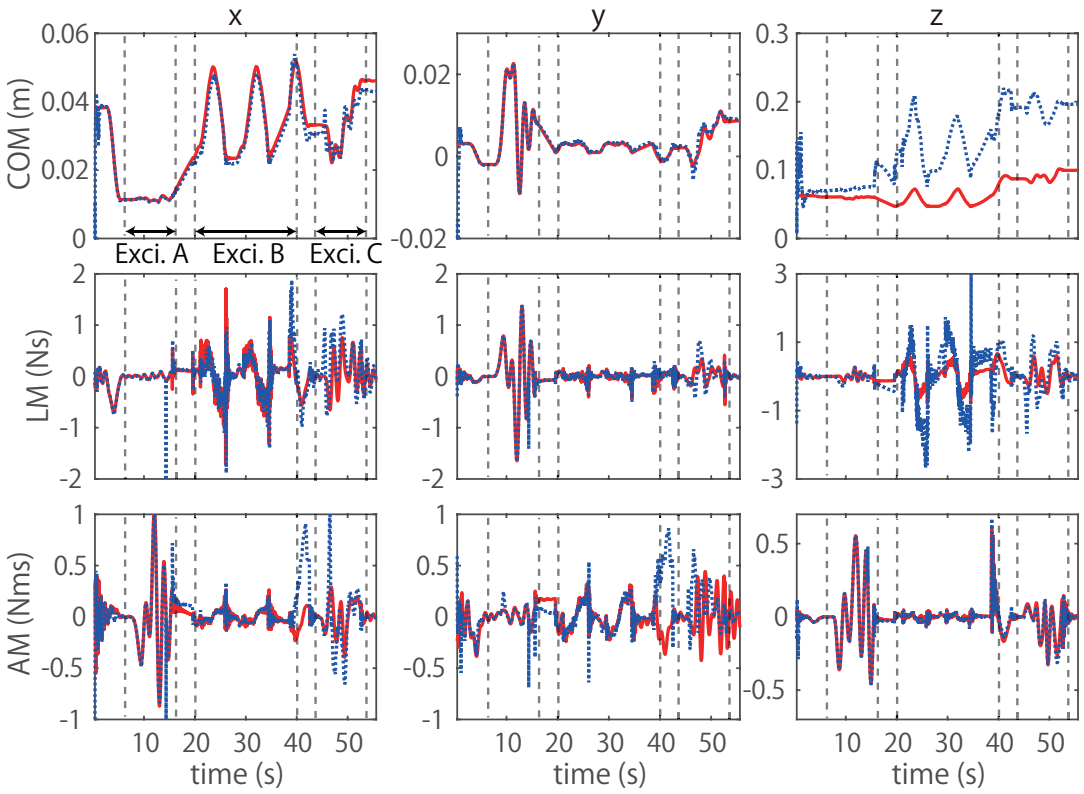

Fig. 3. Simulation results. Center of mass (top row), linear momentum (middle row), and angular momentum (bottom row) time trajectories. X-axis (left col), y-axis (middle col), and z-axis (right col). Red lines denote the true values. Blue dotted lines denote the estimated values. Exci. A is the period for a chest segment exciting motion. Exci. B is the period for a squat motion. Exci. C is the period for arm segments exciting motion.

used the robot sensor values in the simulation environment and the same programming implementation of the real robot for the signal filtering and differential. Figure 4 provides the base link coordinate definition on the robot. In this paper, the initial values of the estimated base parameters are were set to zero in order to check the convergence property of the proposed on-line estimation.

First, we verified the parameter estimation precision. Table I shows the root-mean-square error (RMSE) of the initial 10 s, the final 10 s, and the entire interval of the estimated CoM, LM, and AM. Figure 3 shows the estimated values (Blue dotted lines) after commencement of the identification of the inertial parameters. The values are plotted in the base link (waist link) coordinate. As shown, the RMSE of COM_x and COM_y is less than 3 mm. This result indicates that the values were accurately estimated. Compared to the initial 10 s RMSE and the final 10 s RMSE, the error gradually became smaller, which indicates the precision of the estimated values improved as the robot made more motions.

However, the error for the COM_z increased and finally reached 78 mm. In addition, a comparison of the entire interval RMSE of LM_z with the other LM shows that LM_z is the larger value. Regarding the excitation in the z-axis, the squat motion is the most intense among the test motions. This indicates that only the squat motion is insufficient

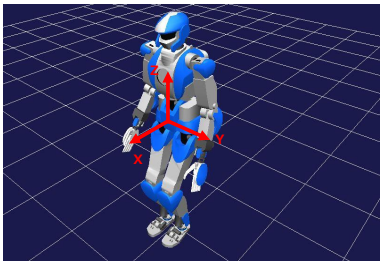

Fig. 4. The base link coordinate definition for the robot

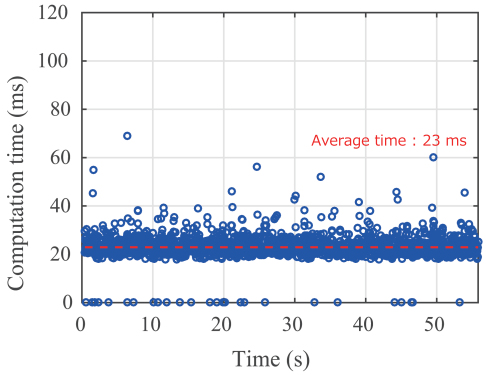

Fig. 5. Computation time of sequential identification at each time instance. Red dotted line denotes the average computation time.

for identification in the z-axis. In previous work of online identification and CoM estimation for humans [9], exciting motion for the z-axis included a push-up motion. As a result, COM_z provided a good performance. Finding a feasible motion that includes sufficient excitation in the z-axis is important future work.

The entire interval RMSE of AM_x is approximately as large as AM_y. AM_x may considerably change when the waist link spins around the y-axis, and an AM_y fluctuation occurs when the link spins around the x-axis. Test motion does not have excitation that includes the waist link. This might be the reason for the errors in AM_x and AM_y.

Next, we verified the computational cost. Figure 5 shows the computational time required for inertial parameter identification and CoM and momentum estimation for each frame. As shown in the figure, the average computing time was 23 ms, and the maximum time was 69 ms. This means the robot can estimate dynamic mass property changes within 10 Hz, which is enough for practical tasks of object manipulation or handling. Thus, the simulation results verified that the proposed method could estimate the online CoM and momentum in a sufficiently precise manner.

TABLE I
THE ROOT-MEAN-SQUARE ERROR (RMSE) OF THE CENTER OF MASS (COM), LINEAR MOMENTUM (LM), AND ANGULAR MOMENTUM (AM) IN THE SIMULATIONS

	COM_x(m)	COM_y(m)	COM_z(m)
RMSE (initial 10 s)	0.01732	0.03736	0.03224
RMSE (final 10 s)	0.00311	0.00037	0.09660
RMSE (entire time)	0.00255	0.00287	0.07799
	LM_x(Ns)	LM_y(Ns)	LM_z(Ns)
RMSE (initial 10 s)	0.12335	0.08312	0.49151
RMSE (final 10 s)	0.03651	0.01302	0.05665
RMSE (entire time)	0.21734	0.09002	0.48519
	AM_x(Nms)	AM_y(Nms)	AM_z(Nms)
RMSE (initial 10 s)	0.64532	0.32717	0.12343
RMSE (final 10 s)	0.01792	0.11671	0.00518
RMSE (entire time)	0.16150	0.22477	0.02019

IV. EXPERIMENTS

To verify that the proposed method detects the CoM fluctuation due to increasing external weights, we conducted experiments for a situation in which the mass properties were intentionally changed. The experiment utilized humanoid robot HRP-4. To verify the estimation precision, the robot recorded the sensor data once, and it was used for CoM estimation using an online method. Figure 6 shows the external weights (each weight was 1.25 kg) and their mounter so that the robot could hold them. Because the mounter was attached to the trunk, the CoM fluctuation occurred when the chest link moved. The position between the chest link and the weight was measured by motion capture. The definitions of the coordinates and identification model are the same as in the simulation. When additional weights were attached on the robot, its motion was usually generated and changed according to the weights to maintain its balance. In this experiment, we used common conservative robot motion, which can be performed by the robot without losing balance in three cases: with no weight, with one weight, and with two weights. The robot repeated the same joint trajectory in all experiments, which had no effect on the CoM fluctuation in any of the three cases. Figure 7 shows photographs of the robot during the experiment. The CoM fluctuation between the three was caused only by the movement of the attached weights, which can be easily calculated by the mass of the weights and their relative position as measured by motion capture.

Figure 8 shows the CoM calculated by CAD data, the external weight position ($CCoM$), and the estimated CoM ($ECoM$) after commencement of identification of the inertial parameters. It should be noted that the initial values of the base parameters used in the sequential identification were all set to zero. Because the inertial parameters from the CAD data are not true values for a real robot, $CCoM$ and $ECoM$ did not entirely match. However, concerning CoM_x and CoM_y, $CCoM$ and $ECoM$ for the same weight have almost similarly shaped trajectories. This result indicates that the CoM estimation succeeded. For more details, we verified the CoM fluctuation, which depends on the number of weights. Table II shows the average CoM fluctuations. In CoMx, the fluctuation of the estimated CoM is very close to the calculated one. Even if two weights are used, the difference is 1.5 mm. $CCoM_y$ and $ECoM_y$ also have similar overall trajectories and the error for the CoM fluctuations between the calculated and estimated values is less than 2.5 mm. The result of CoM_x and CoM_y is within the allowable range for planning or analyzing whole-body motions. $ECoM_z$ is assumed to be insufficient excitation, which is similar to the results of the simulation.

Figure 9 shows the LM and AM calculated by CAD data, and the identified ones. The LM and AM trajectories estimated from the identified values in the latter phase (after around 30 [s]) show the similar patters with respect to those estimated from CAD data. The results indicate that the inertial parameters identification has an effectiveness of estimating the linear/angular momentum of a real robot.

To summarize, the proposed method could appropriately detect the deviation in the CoM caused by the modeling error and the change in the mass property. However, as with the simulation, when the robot excitation motion was insufficient, the estimation did not offer sufficient precision, which supports the importance of well-designed excitation motions.

TABLE II
THE AVERAGE FLUCTUATION OF CENTER OF MASS BETWEEN NO-WEIGHT WITH ONE-WEIGHT (TOP ROW), AND BETWEEN NO-WEIGHT WITH TWO-WEIGHTS (BOTTOM ROW)

	mean(diff. x) (m)	mean(diff. y) (m)	mean(diff. z) (m)
CCoM	0.0091967	0.00012	-0.00946
ECoM	0.0094137	-0.00165	-0.00776
	mean(diff. x) (m)	mean(diff. y) (m)	mean(diff. z) (m)
CCoM	0.0179567	0.00024	-0.01847
ECoM	0.0194788	-0.00117	-0.00511

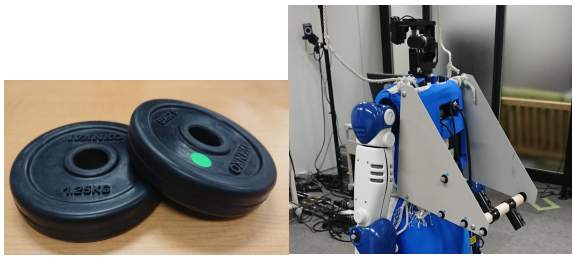

Fig. 6. External weights and weight mounter attached to the chest segments

V. CONCLUSION

We proposed a novel method to estimate the total CoM and momentum using online inertial parameter identification, which is useful for whole-body motion control. The proposed method is based on a real-time identification method for humans. Using only the robot's internal sensors, we executed (1) a separation in the robot link chain and multiple segments for the boundary formed by the force sensor. To achieve online implementation, we executed (2) inertial parameter identification using the sequential least squares method.

The configured system was verified by a dynamic simulation; the result shows that it can cope with changes in mass properties of approximately 10 Hz. The experimental results revealed that the CoM fluctuation due to additional weights can be accurately detected in the horizontal direction. In this environment, the error for CoM fluctuation in the horizontal direction was less than 2.5 mm. The precision is enough for robot control. Because the proposed method utilizes whole-body dynamics, it is possible to estimate various dynamical indices for model-based control. However, we confirmed that the estimation error becomes large for specific estimated values due to a lack of excitation trajectories.

In this study, conservative motion was chosen as the motion for the experiment. Because this excitation is not enough, more dynamic excitation motion is required. If a robot is to execute dynamic motion instead of falling down, it must have accurate mass properties. Nevertheless, mass properties are unknown before their identification. Therefore, in the future, we will construct a motion generation framework in which its motion becomes gradually dynamic and corresponds to the progress of the identification. The detailed accuracy analysis on each identified parameter will be also investigated in our future work.

ACKNOWLEDGMENT

The authors gratefully acknowledge the cooperation of Shimpei Masuda in University of Tsukuba for the experiments using humanoid robot.

REFERENCES

[1] S. Kajita, F. Kanehiro, K. Kaneko, K. Fujiware, K. Harada, K. Yokoi, and H. Hirukawa, "Biped walking pattern generation by using preview control of zero-moment point," *Proc. of the IEEE Int. Conf. on Robots and Automation*, pp. 1620-1626, 2003.

[2] D. Dimitrov, A. Sherikov, and P.-B. Wieber, "A sparse model predictive control formulation for walking motion generation," *Proc. of the IEEE/RSJ Int. Conf. on Intelligent Robots and Systems*, pp. 2292-2299, 2011.

[3] S. Kajita, F. Kanehiro, K. Kaneko, K. Fujiware, K. Harada, K. Yokoi, and H. Hirukawa, "Resolved Momentum Control: Humanoid Motion Planning based on the Linear and Angular Momentum", *Proc. of the IEEE/RSJ Int. Conf. on Intelligent Robots and Systems*, pp. 1644–1650, 2003.

[4] H. Dai, A. Valenzuela and R. Tedrake, "Whole-body Motion Planning with Centroidal Dynamics and Full Kinematics," *Proc. of the IEEE RAS Int. Conf. on Humanoid Robots*, pp. 295-302, 2014.

[5] C. Brasseur, A. Sherikov, C. Collette, D. Dimitrov and P.-B. Wieber, "A Robust Linear MPC Approach to Online Generation of 3D Biped Walking Motion," *Proc. of the IEEE RAS Int. Conf. on Humanoid Robots*, pp. 595-601, 2015.

[6] H. Mayeda, K. Osuka and A. Kangawa, "A New Identification Method for Serial Manipulator Arms," *Proc. IFAC 9th World Congress*, pp.74-79, 1984.

[7] C.G. Atkeson, C.H. An, and J.M. Hollerbach, "Estimation of inertial parameters of manipulator loads and links," *Int. J. of Robotic Research*, vol. 5, no. 3, pp. 101–119, 1986.

[8] K. Ayusawa, G. Venture and Y. Nakamura, "Identifiability and identification of inertial parameters using the underactuated base-link dynamics for legged multibody systems", *Int. J. of Robotics Research*, vol.33, pp.446-468, 2014

[9] G. Venture, K. Ayusawa and Y. Nakamura, "Optimal Estimation of Human Body Segments Dynamics Using Realtime Visual Feedback," *Proc. of the IEEE/RSJ Int. Conf. on Intelligent Robot and System*, pp. 1627-1632, 2009.

[10] K. Ayusawa, G. Venture and Y. Nakamura, "Identification of the Inertial Parameters of a Humanoid Robot Using Unactuated Dynamics of the Base Link," *Proc. of the IEEE RAS Int. Conf. on Humanoid Robots*, pp.1-7, 2008

[11] K. Masuya and T. Sugihara, "COM Motion Estimation of a Humanoid Robot Based on a Fusion of Dynamics and Kinematics Information," *Rroc. of the IEEE/RSJ Int. Conf. on Intelligent Robots and Systems*, pp. 3975-3980, 2015.

[12] S. Piperakis and P. Trahanias, "Non-Linear ZMP based State Estimation for Humanoid Robot Locomotion," *Humanoid Robots (Humanoids), 2016 IEEE-RAS 16th International Conference on*, pp. 202-209, 2016.

[13] J. Carpentier, M. Benallegue, N. Mansard and J. Laumond, "Center of Mass Estimation for Polyarticulated System in Contact - A Spectral Approach," *IEEE Transactions on Robotics*, vol. 32, no. 4, pp. 810-822, 2016.

[14] N. Rotella, A. Herzog, S. Schaal and L. Righetti, "Humanoid Momentum Estimation Using Sensed Contact Wrenches," *Humanoid Robots (Humanoids), 2015 IEEE-RAS 15th International Conference on*, pp. 556-563, 2015.

[15] Y. Fujimoto, S. Obata and A. Kawamura, "Robust Biped Walking with Active Interaction Control between Foot and Ground," *Rroc. of the IEEE Int. Conf. on Robotics and Automation*, pp. 2030-2035, 1998.

[16] H. Kawasaki, Y. Beniya and K. Kanzaki, "Minimum Dynamics Parameters of Tree Structure Robot Models," *Int. Conf. of Industrial Electronics, Control and Instrumentation*, pp. 1100-1105, 1991.

[17] W. Khalil and E. Dombre, "Modeling, identification and control of robots," *Hermes Penton London*, 2002.

[18] K. Kaneko, F. Kanehiro, M. Morisawa, K. Akachi, G. Miyamori, A. Hayashi, and N. Kanehira, "Humanoid robot HRP-4 - Humanoid Robotics Platform with Lightweight and Slim Body - ," *Proc. of the IEEE/RSJ Int. Conf. on Intelligent Robots and Systems*, pp.4400-4407, 2011.

[19] S.Nakaoka, "Choreonoid: Extensible virtual robot environment built on an integrated GUI framework," *Rroc. of the IEEE/SICE Int. Symposium on System and integration*, pp. 79-85, 2012.

[20] K. Ayusawa, A. Rioux, E. Yoshida, G. Venture, and M. Gautier, "Generating persistently exciting trajectory based on condition number optimization," *Rroc. of the IEEE Int. Conf. on Robotics and Automation*, pp. 6518-6524, 2017.

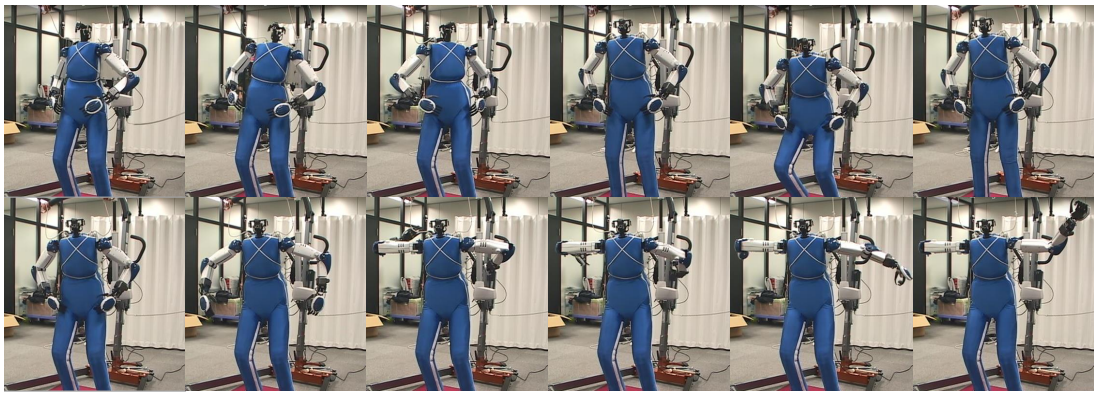

Fig. 7. Photographs of the experiment

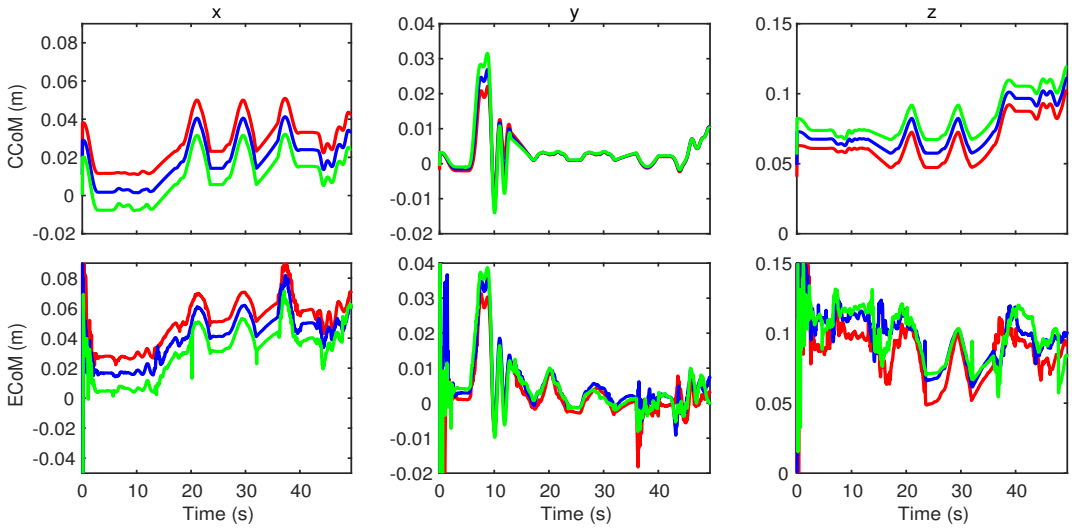

Fig. 8. Experimental results. CoM (Calculated) (top row) and CoM (Estimated) (bottom row). Red lines denote the CoM under no weight. Blue lines denote the CoM under one weight (1.25 kg). Green lines denote the CoM under two weights (2.5 kg).

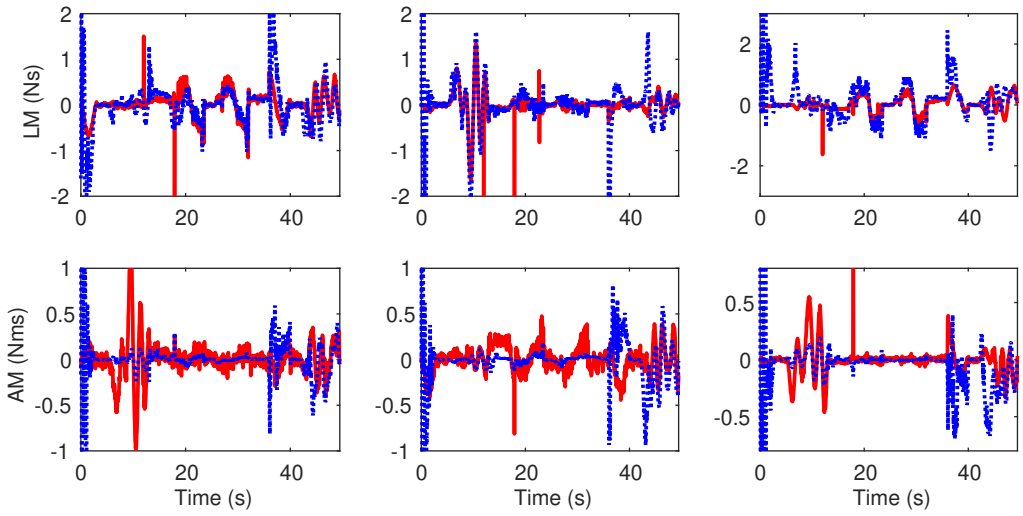

Fig. 9. Experimental results. Linear momentum (top row) and Angular momentum (bottom row) time trajectories with no weights. X-axis (left col), y-axis (middle col), and z-axis (right col). Red lines denote the calculated values from CAD data. Blue dotted lines denote the estimated values.